

**TIME DIFFERENCE OF ARRIVAL ESTIMATION  
USING FAST FOURIER TRANSFORM OVERLAP FOR  
UNDERWATER POSITIONING**

**TAN CHEE SHENG**

**UNIVERSITI SAINS MALAYSIA**

**2019**

**TIME DIFFERENCE OF ARRIVAL ESTIMATION USING FAST FOURIER  
TRANSFORM OVERLAP FOR UNDERWATER POSITIONING**

**by**

**TAN CHEE SHENG**

**Thesis submitted in fulfillment of the  
requirements for the Degree of  
Master of Science**

**June 2019**

## ACKNOWLEDGEMENT

First and foremost, I would like to express my sincerest gratitude to my project main supervisor, Associate Professor Ir. Dr. Rosmiwati binti Mohd Mokhtar for her advice and supervision throughout the progress of master project. I would like to thank for her encouragement and guidance to help me to stay in right path toward the project goal.

My special thanks to core supervisor Professor Ir. Dr. Mohd Rizal bin Arshad for his contribution especially on the idea of the fulfilment of my project. He has been supportive and encouraging through the progress of this project. I appreciate his enthusiasm and willingness. Without which, the project would not have been possible.

I would like to thank all the members of Underwater Robotics Research Group for their helpful guidance to assist me with patience in developing this project. My special thanks reach out to the PhD student, Mr Mad Helmi bin Ab. Majid who is currently doing a project with underwater localization system. He had given me a lot of ideas and guidance whenever I ask for his help.

My grateful thanks also to those who were willing to spend time in assisting me throughout the whole project. Besides, I would also like to give my great appreciation to my beloved friends who always give support and encourage me. Last but not least, I would like to thank to my family that supported me to complete this master project. I truly appreciated them for their kindness in guiding me.

## TABLE OF CONTENTS

	<b>Page</b>
<b>ACKNOWLEDGEMENT</b>	<b>ii</b>
<b>TABLE OF CONTENTS</b>	<b>iii</b>
<b>LIST OF TABLES</b>	<b>viii</b>
<b>LIST OF FIGURES</b>	<b>ix</b>
<b>LIST OF ABBREVIATIONS</b>	<b>xiii</b>
<b>LIST OF SYMBOLS</b>	<b>xvi</b>
<b>ABSTRAK</b>	<b>xviii</b>
<b>ABSTRACT</b>	<b>xix</b>
<b>CHAPTER ONE: INTRODUCTION</b>	
1.1 Background	1
1.2 Motivation	2
1.3 Problem Statements	4
1.4 Research Objectives	5
1.5 Research Scope and Project Limitations	5
1.6 Outlines of Report	6
<b>CHAPTER TWO: LITERATURE REVIEW</b>	
2.1 Introduction	8
2.2 Classes of Positioning System	8
2.3 Positioning Schemes	11
2.3.1 Time of Arrival (TOA)	11
2.3.2 Time Difference of Arrival (TDOA)	12

	<b>Page</b>
2.4 Digital Signal Processing (DSP)	14
2.4.1 Pulse Code Modulation (PCM)	14
2.4.2 Fast Fourier Transform (FFT)	14
2.4.3 Cross-correlation	15
2.4.4 Generalized Cross-correlation with Phase Transform (GCC- PHAT)	17
2.5 Underwater Applications of TDOA	18
2.5.1 AUV Underwater Positioning Algorithm Based on Interactive Assistance of Strapdown Inertial Navigation System (SINS) and Long Baseline (LBL)	18
2.5.2 Robust Target Tracking with Multi-Static Sensors under insufficient TDOA Information	19
2.5.3 A Hybrid Passive Localization Method under Strong Interference with a Preliminary Experimental Demonstration	20
2.5.4 Time Difference of Arrival Estimation Based on Cross Recurrence Plots, with Application to Underwater Acoustic Signals	21
2.5.5 Performance Improvement of TDOA-based Speaker Localization in Joint Noisy and Reverberant Conditions	22
2.5.6 A TDOA Underwater Localization Approach for Shallow Water Environment	23
2.5.7 Moving-Target Position Estimation using Graphics Processing Unit (GPU)-Based Particle Filter for Internet of Things (IoT) Sensing Applications	24

	<b>Page</b>
2.5.8 A Passive Acoustic Positioning Algorithm Based on Virtual Long Baseline Matrix Window	26
2.5.9 Comparison of TDOA	28
2.6 Research Gap	29
2.7 Summary	30
<b>CHAPTER THREE: METHODOLOGY</b>	
3.1 Introduction	31
3.2 Operational Flow and Methodology	32
3.3 Hardware Requirements	34
3.3.1 Raspberry Pi 3 Model B	35
3.3.2 Real Time Clock (RTC)	35
3.3.3 MicroSD Card	36
3.3.4 Pinger	37
3.3.5 Hydrophone	38
3.3.6 USB Sound Card	38
3.3.7 Driver Circuit	39
3.3.8 Preamplifier Circuit	40
3.3.9 Router	41
3.3.10 Li-Po Battery	42
3.4 Software Requirements	42
3.4.1 Putty and Virtual Network Computing (VNC)	43
3.4.2 Gnu Compiler Collection and Integrated Development Environment (IDE)	43

	<b>Page</b>
3.4.3 C and Gnuplot	44
3.4.4 Eagle	44
3.5 Hardware Development	44
3.6 Software Development	46
3.6.1 RTC Module	47
3.6.2 Angle Estimation	48
3.6.3 Network Connection	49
3.6.4 Target Source Positioning Process	50
3.7 Experiment Setup	51
3.7.1 Improved GCC-PHAT Algorithm Test	52
3.7.2 FFT Overlap Algorithm Test	54
3.8 Summary	56
<b>CHAPTER FOUR: RESULTS AND DISCUSSIONS</b>	
4.1 Introduction	57
4.2 Final Prototype	57
4.3 Experimental Results in Open Air	59
4.3.1 Frequency Selection	61
4.3.2 TDOA Algorithms Experimental Test	61
4.3.2(a) Traditional Cross-correlation and Traditional GCC- PHAT	62
4.3.2(b) Improved Cross-correlation and Improved GCC- PHAT	63
4.3.2(c) Proposed FFT Overlap	69

	<b>Page</b>
4.3.3 Comparison of Performance for TDOA Estimation between Five Different Algorithms	72
4.4 Underwater Experimental Results	74
4.5 Comparison of Results based on Improved GCC-PHAT and Proposed FFT Overlap Algorithms	80
4.6 Summary	81
 <b>CHAPTER FIVE: CONCLUSION AND FUTURE WORKS</b>	
5.1 Conclusion	82
5.2 Future Works	83
 <b>REFERENCES</b>	 <b>84</b>
 <b>APPENDICES</b>	
Appendix A: The Specifications of Raspberry Pi 3 Model B	
Appendix B: The Specifications of U-Green 2-in-1 USB External Audio Adapter	
 <b>LIST OF PUBLICATIONS</b>	



## LIST OF TABLES

		<b>Page</b>
Table 2.1	Baselines length (Vickery, 1998).	10
Table 2.2	Comparison of the different measurement approaches.	28
Table 3.1	Main hardware components of the underwater positioning system.	34
Table 3.2	Connection of the DS 3231 real time clock with the Raspberry Pi 3.	47
Table 4.1	Comparison of accuracy for TDOA estimation based on different percentages of overlap.	71
Table 4.2	Experimental results of the TDOA estimation based on five different algorithms.	72
Table 4.3	Comparison of computational time for TDOA estimation based on five different algorithms.	73
Table 4.4	Comparison of percentage error for TDOA estimation based on five different algorithms.	73
Table 4.5	Results of angle estimation according to the position A.	78
Table 4.6	Results of angle estimation according to the position B.	78
Table 4.7	Summary of the advantages and the disadvantages based on improved GCC-PHAT and FFT overlap (100%) algorithms.	80

## LIST OF FIGURES

		<b>Page</b>
Figure 1.1	Underwater communication system (Bjørnø, 2017).	2
Figure 2.1	Positioning systems. (a) LBL, (b) SBL, (c) USBL (Paull <i>et al.</i> , 2017).	9
Figure 2.2	Bilateration using the geometry of circles (Askari and Bareket, 2017).	11
Figure 2.3	Hyperbolic multilateration (Gustafsson and Gunnarsson, 2013).	13
Figure 2.4	Block diagram of the GCC-PHAT function (Hosseini <i>et al.</i> , 2017).	17
Figure 2.5	Integrated navigation system using SINS, DVL, MCP and LBL (Zhang <i>et al.</i> , 2015).	19
Figure 2.6	Fusion of the TDOA measurement (Shin <i>et al.</i> , 2018).	20
Figure 2.7	Results of localization based on TDOA measurement (a) with interference cancellation, (b) without interference cancellation (Lei <i>et al.</i> , 2016).	21
Figure 2.8	TDOA estimation using the CRP matrix (Bot <i>et al.</i> , 2016).	22
Figure 2.9	Performance of 3D localization in a room (Abutalebi and Momenzadeh, 2011).	23
Figure 2.10	Delay Doppler map (3D correlation function) (Kouzoundjian <i>et al.</i> , 2017).	24
Figure 2.11	GPU accelerated FFT parallel computing (Kim <i>et al.</i> , 2017).	25
Figure 2.12	GPU accelerated particle filter parallel computing (Kim <i>et al.</i> , 2017).	25
Figure 2.13	Virtual matrix window model (Zhang <i>et al.</i> , 2018).	26
Figure 2.14	The plot of GCC-SCOT function (Zhang <i>et al.</i> , 2018).	27
Figure 3.1	Design flow chart.	33
Figure 3.2	Mechanical structure on the floating boat.	34
Figure 3.3	Raspberry Pi (RPi) 3 model B.	35

	<b>Page</b>	
Figure 3.4	DS 3231 real time clock (RTC).	36
Figure 3.5	MicroSD card class 10 with adapter.	36
Figure 3.6	Pinger.	37
Figure 3.7	Hydrophone.	38
Figure 3.8	U-Green 2-in-1 USB external sound audio adapter.	39
Figure 3.9	Driver circuit schematic diagram.	39
Figure 3.10	Completed driver PCB.	40
Figure 3.11	Preamplifier circuit schematic diagram.	40
Figure 3.12	Completed preamplifier PCB.	41
Figure 3.13	TP-Link 150 Mbps wireless N router.	41
Figure 3.14	3-cells and 4-cells Li-Po batteries.	42
Figure 3.15	Block diagram of the overall hardware system.	45
Figure 3.16	Software development process.	47
Figure 3.17	Angle estimation of the signal at the hydrophone pair.	48
Figure 3.18	Socket connection between client and server.	49
Figure 3.19	Flow chart of positioning system.	51
Figure 3.20	Flow chart of GCC-PHAT based on segmentation.	53
Figure 3.21	Data string in time series. (a) No overlap, (b) 50% overlap, (c) Fully overlap.	54
Figure 3.22	Flow chart of FFT overlap based on segmentation.	55
Figure 4.1	Completed hardware prototype. (a) Transmitter module, (b) Receiver module.	58
Figure 4.2	Bottom view of ASV buoy.	59
Figure 4.3	Experimental setup in open air.	60
Figure 4.4	SNR performance. (a) Hydrophone 1, (b) Hydrophone 2.	61

		<b>Page</b>
Figure 4.5	Signals recorded in open air environment. (a) Received signal 1, (b) Received signal 2.	62
Figure 4.6	Experimental results. (a) Traditional cross-correlation, (b) Traditional GCC-PHAT.	63
Figure 4.7	Signals are divided into the several segments with a 1024 samples. Received signal 1, (a) 1st segment (0-1023 samples), (b) 2nd segment (1024-2047 samples), (c) 3rd segment (2048-3071 samples), (d) 4th segment (3072-4095 samples).	64
Figure 4.7	Signals are divided into the several segments with a 1024 samples. Received signal 2, (e) 1st segment (0-1023 samples), (f) 2nd segment (1024-2047 samples), (g) 3rd segment (2048-3071 samples), (h) 4th segment (3072-4095 samples) (continued).	65
Figure 4.8	Performing the FFT processing on all segments. (a) Frequency spectrum of received signal 1, (b) Frequency spectrum of received signal 2.	66
Figure 4.9	Rearrangement of the selected segments. (a) Received signal 1, (b) Received signal 2.	67
Figure 4.10	Experimental results. (a) Improved cross-correlation, (b) Improved GCC-PHAT.	68
Figure 4.11	Results of time delay estimation. (a) Improved cross-correlation, (b) Improved GCC-PHAT.	68
Figure 4.11	Experimental results of the proposed FFT overlap. Received signal 1, (a) 0% overlap, (c) 50% overlap. Received signal 2, (b) 0% overlap, (d) 50% overlap.	69
Figure 4.12	Experimental results of the proposed FFT overlap. Received signal 1, (e) 75% overlap, (g) 100% overlap. Received signal 2, (f) 75% overlap, (h) 100% overlap (continued).	70
Figure 4.13	Results of time delay estimation using segmentation, FFT overlap and peak detection.	71
Figure 4.14	Experimental setup in pool.	74
Figure 4.15	Experimental setups in 6 different positons. (a) Top view, (b) Side view.	75
Figure 4.16	Signal received. (a) Left hydrophone, (b) Right hydrophone.	76

	<b>Page</b>	
Figure 4.17	Experimental results of the position estimation by using the improved GCC-PHAT. The number of samples lag (a) -2, (b) -1.	76
Figure 4.17	Experimental results of the position estimation by using the improved GCC-PHAT. The number of samples lag (c) 0, (d) 1 (continued).	77
Figure 4.18	Experimental results of the FFT overlap at 16.5 kHz. (a) Signal received from left hydrophone, (b) Signal received from right hydrophone.	77
Figure 4.19	Results of experiment according to the position A by using the FFT with 100% overlap. Angle estimation at (a) Left ( $-55^\circ$ ), (b) Center ( $0^\circ$ ), (c) Right ( $55^\circ$ ).	79

## LIST OF ABBREVIATIONS

2D	2 Dimensions
3D	3 Dimensions
ARM	Advance RISC Machines
ADC	Analog-to-Digital Converter
AUV	Autonomous Underwater Vehicle
ASV	Autonomous Surface Vehicle
CSI	Camera Serial Interface
CRP	Cross-Recurrence Plot
DDM	Delay Doppler Map
DSP	Digital Signal Processing
DAC	Digital-to-Analog Converter
DFT	Discrete Fourier Transform
DVL	Doppler Velocity Log
FFT	Fast Fourier Transform
GMM	Gaussian Mixture Model
GPIO	General Purpose Input/ Output
GCC	Generalized Cross Correlation
GPS	Global Positioning System
GIB	GPS Intelligent Buoy
GUI	Graphical User Interface
GPU	Graphics Processing Unit
GND	Ground

I/O	Input/Output
IC	Integrated Circuit
IDLE	Integrated Development and Learning Environment
IDE	Integrated Development Environment
I <sup>2</sup> C	Inter-Integrated Circuit
IoT	Internet of Things
IP	Internet Protocol
iSBL	Inverted Short Baseline
Li-Po	Lithium ion Polymer
LAN	Local Area Network
LBL	Long Baseline
MCP	Magnetic Compass Pilot
ML	Maximum Likelihood
MSS	Multi-Static Sonar System
OS	Operation System
PHAT	Phase Transform
PCB	Printed Circuit Board
PCM	Pulse Code Modulation
RF	Radio Frequency
RAM	Random-Access Memory
RPi	Raspberry Pi
RTC	Real Time Clock
RSS	Received Signal Strength
RQA	Recurrence Quantification Analysis

RISC	Reduced Instruction Set Computer
SD	Secure Digital
SSH	Secure Shell
SCL	Serial Clock Line
SDA	Serial Data Line
SBL	Short Baseline
SNR	Signal-to-Noise Ratio
SCOT	Smooth Coherent Transform
SQW	Square Wave
SINS	Strapdown Inertial Navigation System
TXCO	Temperature-Compensated Crystal Oscillator
TDE	Time Delay Estimation
TDOA	Time Difference of Arrival
TOA	Time of Arrival
USBL	Ultra-Short Baseline
USB	Universal Series Bus
UUV	Unmanned Underwater Vehicle
VNC	Virtual Network Computing
Wi-Fi	Wireless Fidelity



## LIST OF SYMBOLS

$X$	Actual value
$\theta$	Angle in degree
$\omega$	Angular frequency
$A$	Amplitude of signal
$R(\omega)$	Cross-spectral density function
$\hat{\tau}$	Delay based on the maximum value in cross correlation function
$k$	Discrete frequency
$n$	Discrete time
$z$	Discrete time samples
$d, D$	Distance
$\varepsilon$	Error
$\eta$	FFT length
$S_{FFT}$	First of the two segments that contain frequency of interest
$X(k)$	Fourier transform as a function of the discrete frequency, $k$
$\emptyset(\omega)$	Frequency weighting function
$h(\omega)$	Hamming window function
$\alpha$	Integer depending on the types of overlap percentage for computing FFT
$x$	Input signal
$\varphi$	Lag

$(x, y)$	Location
$\bar{Y}$	Mean value
$Y$	Measured value
$\gamma$	Noise signal
$N$	Number of discrete points in time/frequency
$r(\tau)$	Output of cross correlation within a range, $\tau$
$\emptyset$	Phase signal
$N_{FFT}$	Position number of FFT
$y$	Receiving signal
$f_s$	Sampling rate
$f$	Signal frequency
$s$	Source signal
$c$	Speed of sound
$\tau$	Time delay
$t_d$	Time delay in the discrete form
$N_i$	Total number of samples in a segment

**PENGANGGARAN BEZAAN MASA KETIBAAN MENGGUNAKAN  
JELMAAN FOURIER PANTAS SECARA PERTINDIHAN BAGI PENENTU  
KEDUDUKAN BAWAH AIR**

**ABSTRAK**

Projek ini membentangkan sistem penentu kedudukan bawah air dengan menggunakan pengukuran bezaan masa ketibaan (TDOA). Dalam penyelidikan ini, alat perhubungan bawah air dibina dan algoritma jelmaan Fourier pantas (FFT) secara pertindihan dicadangkan bagi mencapai tujuan projek ini. Teknik TDOA digunakan untuk menganggar kedudukan sasaran bawah air. Penganggaran TDOA diperolehi berdasarkan kekuatan isyarat yang diterima dengan frekuensi yang diinginkan. Pengekstrakan isyarat daripada penerima dilakukan dengan menggunakan algoritma pemprosesan isyarat digital. FFT digunakan untuk menukar isyarat yang diterima daripada domain masa kepada domain frekuensi bagi mengekstrak maklumat isyarat (frekuensi dan amplitud berkaitan). Oleh itu, penganggaran TDOA boleh diperolehi daripada maklumat frekuensi dengan menggunakan pemprosesan jelmaan bertindih. Keputusan eksperimen dipersembahkan demi menunjukkan keupayaan algoritma yang dicadangkan. Keputusan menunjukkan FFT yang dicadangkan dengan 100% pertindihan telah berjaya meningkatkan ketepatan dengan peratus ralat sebanyak 1.71% sahaja bagi penganggaran TDOA. Secara keseluruhan, sistem penentu kedudukan dengan menggunakan FFT secara pertindihan berupaya untuk memberikan anggaran kedudukan yang tepat.

# **TIME DIFFERENCE OF ARRIVAL ESTIMATION USING FAST FOURIER TRANSFORM OVERLAP FOR UNDERWATER POSITIONING**

## **ABSTRACT**

This project presents an underwater acoustic positioning system based on time difference of arrival (TDOA) measurement. In this research, an underwater communication device is developed and fast Fourier transform (FFT) overlap algorithm is proposed in order to achieve the objectives. The TDOA technique is used to estimate the position of an underwater target. The TDOA estimation is derived based on the intensity of a received signal with the frequency of interest. An extraction of a signal from a receiver is performed by using digital signal processing algorithms. The FFT is used to convert the receiving signal from time domain into frequency domain for extraction of the signal information (relevant frequency and amplitude). Hence, the TDOA estimation can be obtained from the frequency information using an overlap transform processing. Experimental results are presented to demonstrate the capabilities of the proposed algorithms. The results indicate that the proposed FFT with 100% overlap has successfully improved an accuracy with percentage error of 1.71% for the TDOA estimation. Overall, the positioning system using FFT overlap able to provide an accurate positioning estimation.

# CHAPTER ONE

## INTRODUCTION

### 1.1 Background

An underwater acoustic is the study of sound in the water that encompass not only about sound propagation, but also the masking of sound signals by an interfering phenomenon. It also includes a study of signal processing for extracting these signals from an interference (Kuperman and Roux, 2014; Lurton, 2010). The underwater acoustic uses sound source to learn about a physical and a biological characteristics of the lake, river or sea. An acoustic wave propagates better than an electromagnetic wave in an underwater applications (Arshad, 2009). This is due to the transmission of an electromagnetic wave suffers from a strong attenuation through the underwater. Therefore, the underwater acoustic is a very important vector in an underwater communication system, localization system and positioning system (Choi *et al.*, 2017; Majid and Arshad, 2016; Sasano *et al.*, 2016).

The underwater acoustic positioning system is important for navigation and tracking of an underwater vehicles such as unmanned underwater vehicle (UUV) or autonomous underwater vehicle (AUV). The system provides an information of the underwater object when a communication is established over an acoustic link in sonar systems as shown in Figure 1.1. Positioning system requires high accuracy in measurement that enables target identification and tracking. It is necessary to consider about the number of underwater devices, operation range and time.

A sonar has been widely used in an environment monitoring, obstacle avoidance system and an underwater object detection (Du *et al.*, 2017; Galarza *et al.*,

2016). The sonar transducer which is also known as ultrasonic sensing, is a device that has been used for extracting the information by using propagation of acoustic energy (Kleeman and Kuc, 2016). Commonly, the frequencies are in the range of 20 kHz to 100 kHz. It typically mounted on AUV to detect an underwater objects. The higher frequency of ultrasonic leads to higher accuracy of the distance measurement. However, high ultrasonic frequency works only at short range (Zhou *et al.*, 2018).

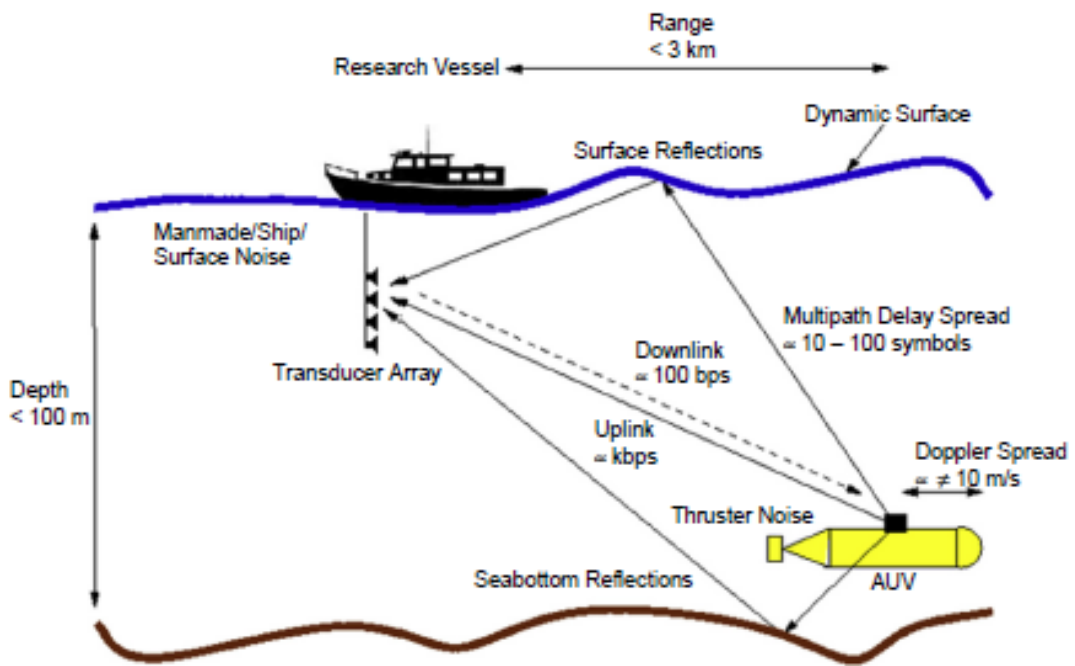


Figure 1.1. Underwater communication system (Bjørnø, 2017).

## 1.2 Motivation

A development of the underwater system and the technology in Malaysia is still progressing and there are still many areas that related to the marine science and the ocean engineering that are not fully utilized. The underwater observation is one of an example. Via this research, the underwater observation system and a network are investigated as well as the acoustic positioning system will be developed. An outcome will provide a significant contribution for the marine oceanographic data for research,

localization, monitoring and search and rescue mission in our country. Furthermore, it also help to improve the safety and protect the marine environment in our country knowingly that Malaysia is being surrounded with an ocean.

An autonomous surface vessel (ASV) has potential and great benefit to the environment. It operates on the surface of the water so they are best suited for measurements and data collection. Many scientists and researchers need a system to collect a data on the ocean such as satellite systems and floating buoys. However, the data collection is limited due to the cost of the satellite systems. Hence, the ASV can solve the problem to help collecting the environmental data. The ASV might be able to collect the new ocean data in any situation. The ASV technology has been improved and being researched so as to be used in an environmental monitoring.

The distance between the transmitter and receiver using ultrasonic sensor is measured based on time-of-arrival (TOA) (Biao and Cheng, 2018; Casey *et al.*, 2007; Diamant *et al.*, 2016) and time-different-of-arrival (TDOA) (Abutalebi and Momenzadeh, 2011; Shome, 2015; Valente and Alves, 2016). Time of arrival (TOA) technique uses the arrival time from transmitter to receiver to measure distance. The measured distance is determined based on set of circles. On the other hand, time difference of arrival (TDOA) method determines the location from the differences of the arrival time on a pair of receivers. It is typically obtained by an intersection of a multiple hyperbolic curves. Both of them have provided a high accuracy for the underwater positioning system.

### 1.3 Problem Statements

A main challenging task of a navigation system and a tracking system for an UUV is to obtain precise and accurate position measurement. Currently, the positioning of a mobile robot in air is using a global positioning system (GPS) technique. Due to a poor penetration of the GPS signal, it fails to operate underwater. Hence, the acoustic communication is used to perform the underwater positioning and the localization. For instance, a GPS intelligent buoy (GIB) system (Alcocer *et al.*, 2006; Alcocer *et al.*, 2007; Xin *et al.*, 2018) is a combination of the GPS and the acoustic communications between a satellites, ground based station, floating buoys and underwater targets. However, there is still a lot of research to be done in the underwater acoustic positioning system. In order to identify the position of the UUV, the system requires an accurate location of the network of floating buoys.

The TDOA estimation based on generalized cross-correlation (GCC) has been widely utilized in the underwater positioning and the localization system (Valente and Alves, 2016). A sharpen peak of a correlation between two signals represent time lag between them. An accuracy is improved as compared to a traditional cross-correlation (Chen *et al.*, 2006). However, a disadvantage of utilizing the GCC for the TDOA estimation is that it is easily influenced by a noise and reverberation (Abutalebi and Momenzadeh, 2011). The effect of noise and reverberation on the GCC method can lead to poor TDOA estimation. It is the most significant challenge for the position measurement.



## **1.4 Research Objectives**

The aim of this study is to utilize the time of difference arrival algorithm to estimate the directional angle of the underwater target. This is fulfilled by the following objectives:

1. To design and develop an acoustic instrumentation tool for underwater measurement and positioning.
2. To propose the fast Fourier transform overlap algorithm for time difference arrival estimation.

## **1.5 Research Scope and Project Limitations**

The first stage involve the development of the ASV platform. This involve an implementation of the software interfaces using the hardware platform. A Raspberry Pi (RPi) is used as a main control unit for integration of all sensors and components with a laptop. A pinger and hydrophones are designed by using a piezoelectric element. The components such as sound card and preamplifier module are used for audio signal processing. Two sound cards attached on one RPi instead of using two RPi's due to the project is carried out without using the GPS module. All components used limited their performance. Therefore, the performance may be different but it still able to provide with accurate position estimation in a real environment.

An experiment is carried out in only a controlled environment such as swimming pool. The location of the hydrophones and pinger is set to 3 m baseline and 2.2 m depth. This is due to the depth of the swimming pool is 2.2 m and the maximum allowable baseline for the hydrophones is 3 m only. The wind, current and wave

disturbance are not taken into consideration in this experiment. This is because the experiment is assumed to be carried out in calm water condition without dynamic changes of water environment. In addition, the change in sound velocity due to change in pressure (depth) and temperature is assumed to be negligible. The velocity of sound in water is taken as 1484 m/s.

Assumptions have been made regarding the acoustic source and hydrophones that are used in this project. Single sound source and hydrophones are small and omnidirectional. The reflections of acoustic source from the surrounding objects and pool tiles are negligible. The target source to be located, is kept stationary during the data acquisition process. Hydrophones are assumed to be both phase and amplitude matched and without self-noise. The positions of hydrophones to be located are known and the baseline length is fixed.

Furthermore, the target position to be estimated is based on angle measurement relative to the baseline.

## **1.6 Outlines of Report**

This thesis consists of five main chapters. In chapter 1, it is an introduction chapter that discusses a background of the underwater acoustic positioning system, motivation, problem statement, objectives and scope of this project. Chapter 2 will discuss a literature reviews that have been done. It will discuss about classes of the positioning system and positioning schemes. Other than that, the previous works on applications of TDOA estimations in the underwater field of localization and positioning are reviewed. In addition, several types of the TDOA estimation based on different measurement approaches are reviewed.

In Chapter 3, the discussions will be on methodology, hardware and software implementation of this project. A mechanical drawing and a design of hardware are stated. All steps involved and the algorithms are explained in detail in this chapter. Besides that, two types of time delay estimation (TDE) approaches are discussed such as improved GCC-PHAT and FFT overlap.

The results and discussions will be presented in Chapter 4. Section 4.2 shows the completed hardware platform of ASV. Both tables and figures are used to illustrate concepts and to present the results in a detailed and readable way. Last but not least, Chapter 5 discusses the conclusion of this project and the future work or research improvements that can be done.

## **CHAPTER TWO**

### **LITERATURE REVIEW**

#### **2.1 Introduction**

This chapter discusses on several activities for fundamental understanding on the underwater acoustic positioning system. A brief overview of the positioning methods including the classes of the positioning system and its measurement are explained in this chapter. A bilateration and a multilateration techniques based on location method as well as its performances are also discussed. This chapter also aims to investigate different technologies and methods used for underwater positioning system and localization system.

#### **2.2 Classes of Positioning System**

The positioning system can be classified into three classes; long baseline (LBL) system (Han *et al.*, 2015; Thomson *et al.*, 2018; Zhang *et al.*, 2018), short baseline (SBL) system (Smith and Kronen, 1997; Zhai *et al.*, 2009) and ultra-short baseline (USBL) system (Reis *et al.*, 2016; Rypkema *et al.*, 2017; Sun *et al.*, 2014) as shown in Figure 2.1. Those systems consist of the transmitters and the receivers to measure the positions relative to a reference point by measuring the time of arrival (TOA) or the time different of arrival (TDOA).

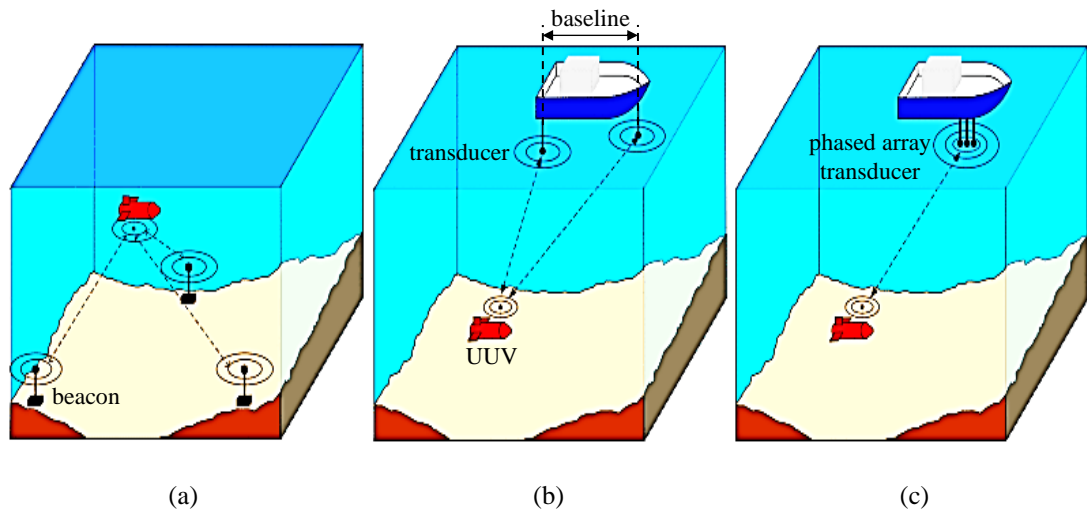


Figure 2.1. Positioning systems. (a) LBL, (b) SBL, (c) USBL (Paull *et al.*, 2017).

The LBL system is the most accurate system as compared to the SBL and the USBL systems due to a fixed underwater beacons installation on a sea floor (Jakuba *et al.*, 2008). However, it has higher installation time and cost as well as the operation area is limited by the small amount of beacons. The SBL system requires 3 or more transducers that typically mounted on the ship. It receives signals from the underwater unit and records the time taken for each transducer. This system will have poor positioning accuracy if the baseline length is less than 20 m.

On the other hand, the USBL system needs an array of transducers to install on the small boat. It receives a phase delay of signal to determine the location of target. Both of the SBL and the USBL systems have good range of accuracy but it depends on a baseline length (Christ and Wernli, 2013). An Inverted SBL (iSBL) system is suggested by Stovner and Johansen (2018) for underwater position estimation. This system requires only one underwater beacon that installed on the seabed instead of three beacons that are used in the LBL system. Thus, the iSBL system helps to reduce the deployment and maintenance cost of beacons by approximately 50 % as compared to LBL system.

Furthermore, the GPS intelligent buoy (GIB) system is another current technology which is based on network of floating buoys (Wang *et al.*, 2016). The relative coordinates of the onboard hydrophones are obtained with accurate timing on the GPS. The system reduces the deployment and calibration time due to the buoys are operated on the water surface. This system provides real time of the underwater multi-targets tracking due to simplex communication between the floating buoys and the underwater targets (Choi and Yuh, 2016). The disadvantages of this system are similar to the LBL system since the operation area depends on the fixed range of each floating buoys. Therefore, there is limitation of the operation area and it requires time for buoys to move from one place to another.

The significant difference between these systems is the baseline length with its location of transducers. The LBL system has longest baseline up to 6 km which is widely used for long range tracking mission. The SBL system only operates from range between 20 m to 50 m, the position accuracy can be achieve within several meters for a maximum operation range. In the USBL system, it requires the array of transducers with compact baseline sensor array configuration. It has shortest baseline length in order to avoid ambiguity in phase angle measurement. Table 2.1 shows three categories of acoustic positioning system according to the length of the baselines.

Table 2.1: Baselines length (Vickery, 1998).

<b>Types of Underwater Acoustic Positioning System</b>	<b>Baseline Length</b>
Long baseline (LBL)	100 m ~ 6000 m
Short baseline (SBL)	20 m ~ 50 m
Ultrashort baseline (USBL)	< 10 cm

## 2.3 Positioning Schemes

Most common method for the underwater positioning is range-based with time-only positioning such as TOA and TDOA. It estimates the position of the underwater targets by exploiting the relations between the transmitters and the receivers. This technique utilize the time and the range measurements include distance and angle estimation.

### 2.3.1 Time of Arrival (TOA)

The TOA method measures the arrival time with a distance calculation to estimate the position of underwater target by using bilateration or trilateration technique (Klungmontri *et al.*, 2015). Bilateration is the process of finding intersection point in two dimensional (2D) space whereas trilateration provides the coordinates in three dimensional (3D) space. The principle of the bilateration is illustrated as shown in Figure 2.2.

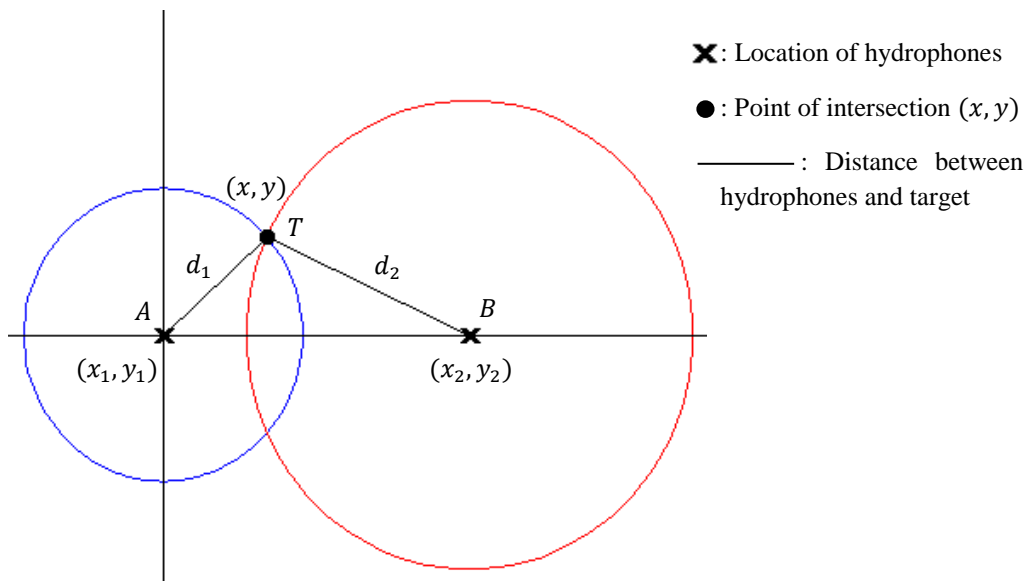


Figure 2.2. Bilateration using a geometry of circles (Askari and Bareket, 2017).

Suppose two points  $A(x_1, y_1)$  and  $B(x_2, y_2)$  in 2D space, the point of intersection  $T(x, y)$  is represent the position of the target and the distance from the target  $T$  to points A and B are  $d_1$  and  $d_2$  respectively. Two equations are obtained based on the bilateration as in (2.1) and (2.2) (Askari and Bareket, 2017),

$$(x - x_1)^2 + (y - y_1)^2 = d_1^2 \quad (2.1)$$

$$(x - x_2)^2 + (y - y_2)^2 = d_2^2 \quad (2.2)$$

Assume two points (point A and point B) are located at  $(0,0)$  and  $(x_2, 0)$  respectively, the position  $x$  and  $y$  can be calculated using an Equation (2.3) and (2.4) (Askari and Bareket, 2017).

$$x = \frac{d_1^2 - d_2^2 + x_2^2}{2x_2} \quad (2.3)$$

$$y = \sqrt{d_1^2 - x^2} \quad (2.4)$$

where  $x_2 > 0$ .

### 2.3.2 Time Difference of Arrival (TDOA)

The TDOA is measured by a hyperbolic positioning using multilateration technique. It is based on distance differences between numbers of points to determine the position of target. The geometry of the TDOA position in 2D space is shown in Figure 2.3. The time difference arrival with distance difference between two points to the target source can be obtained as in (2.5) (Gustafsson and Gunnarsson, 2013).

$$d_1 - d_2 = (\tau_1 - \tau_2)c \quad (2.5)$$



where  $d_1$  is the length between point  $A$  and target  $T$ ,  $d_2$  is the length between point  $B$  and target  $T$ ,  $c$  is the speed of transmitted signal,  $(\tau_1 - \tau_2)$  is the time difference when the signal reaches point  $A$  and point  $B$  respectively.

The distance difference is defined as a hyperbolic function with two focal points. An intersection point from the hyperbolas is determined in 2D space as shown in Figure 2.3. Consider in two points, the location of target  $T(x, y)$  can be obtained from Equation (2.6) according to Figure 2.3 (Gustafsson and Gunnarsson, 2013).

$$d_1 - d_2 = \sqrt{y^2 + \left(x + \frac{D}{2}\right)^2} - \sqrt{y^2 + \left(x - \frac{D}{2}\right)^2} \quad (2.6)$$

where  $D$  is the distance between point  $A$  and point  $B$  at fixed location. However, it is difficult to find the position of target since only two lateration are considered. The relationship between  $x$  and  $y$  as shown in Equation (2.7).

$$y = \pm \sqrt{\frac{D^2 - (d_1 - d_2)^2}{4} - \frac{(d_1 - d_2)^2}{4}} x \quad (2.7)$$

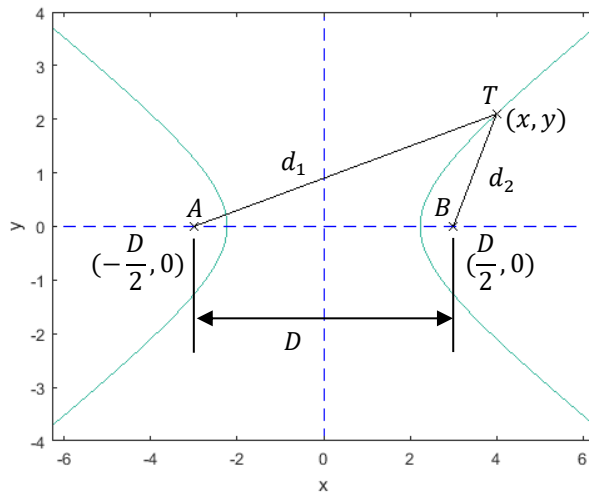


Figure 2.3. Hyperbolic multilateration (Gustafsson and Gunnarsson, 2013).

## **2.4 Digital Signal Processing (DSP)**

Traditionally, the signals are processed analogically for a continuous time system (Camps-Valls *et al.*, 2018). It is essential to extract the information from an input signal. The development of digital computer and microprocessor leading to digital signal processing (DSP) has become an important technique for real time applications. DSP provides greater flexibility, software reproducibility and reliability as well as solving computational complexity (Kuo *et al.*, 2013).

### **2.4.1 Pulse Code Modulation (PCM)**

Pulse code modulation (PCM) is a digital processing technique that converts an analog audio signal into digital form. The analog signal is continuously sampled at certain sampling rate, then being quantized into digital binary code sequence. The signal resolution is dependent on sampling rate and the bit depth (Newmarch, 2017). Most modern sound cards have built-in analog to digital converter (ADC) that can perform PCM.

### **2.4.2 Fast Fourier Transform (FFT)**

Fast Fourier transform (FFT) is an efficient implementation of discrete Fourier transform (DFT) that translate acoustic signal of time domain into frequency domain on modern digital computation (Vaingast, 2014). FFT manages to reduce the complexity that scales linearly with respect to the size of FFT bins. The FFT algorithm

plays an important role in various applications such as linear filtering, correlation and spectrum analysis.

The FFT was originally developed by Gauss in 1805. However, his work did not analyze an asymptotic computational time. The FFT algorithm has been developed and become popular after the paper is published in 1965 by Cooley and Tukey (Heiderman *et al.*, 1984). It reduces the computational time by reducing the number of complex multiplications compared to DFT. The DFT of discrete  $N$ -point sequence  $x(n)$  is denoted by  $X(k)$  as in (2.8).

$$X(k) = \sum_{n=0}^{N-1} x(n) \omega_N^{nk} \quad (2.8)$$

where  $\omega_N = e^{-j2\pi/N}$  is a primitive root of unit and  $0 \leq k \leq N - 1$ . The computational complexity based on DFT needs  $N^2$  complex multiplications and  $N(N - 1) \cong N^2$  complex addition to obtain a complete set of its coefficients. On the other hand, the evaluation of the FFT algorithm requires  $N \log_2 N$  operation that it helps to reduce the DFT operation numbers. Thus, the implementation of FFT is faster than DFT if the value of  $N$  is large.

### 2.4.3 Cross-correlation

The cross-correlation refers to the similarity between two signals received from different time delay (Kumar, 2013). The time delay estimation using cross-correlation method is briefly described as follows. Let  $x_1(t)$  and  $x_2(t)$  as the signals received from two hydrophones, the continuous time signals are converted into the discrete signals,  $x_1[n]$  and  $x_2[n]$  by sound cards as shown in Equation (2.9) and (2.10).

$$x_1[n] = s[n] + \gamma_1[n] \quad (2.9)$$

$$x_2[n] = s[n + t_d] + \gamma_2[n] \quad (2.10)$$

where  $t_d$  is the time delay in the discrete form,  $s[n]$  is the source signal,  $\gamma_1[n]$  and  $\gamma_2[n]$  are the noise induced by surrounding. The discrete signals are further processed with a hamming window to reduce spectral leakage. The cross-correlation between two continuous time signals is given by (2.11).

$$r_{x_1, x_2}(\tau) = \int_{-\infty}^{\infty} x_1(t) x_2^*(t + \tau) dt \quad (2.11)$$

where  $x_2^*(t)$  is the complex conjugate of  $x_2(t)$  and  $\tau$  is the time delay between two signals. However, the direct evaluation of cross-correlation in time domain requires high processing time as compared to cross-correlation based on FFT (Zhang, Z. M., 2018). The next Equation (2.12) shows the cross-correlation by applying FFT.

$$\begin{aligned} R_{x_1, x_2}(\omega) &= \int_{-\infty}^{\infty} r_{x_1, x_2}(\tau) e^{-i\omega\tau} d\tau \\ &= X_1(\omega) X_2^*(\omega) \end{aligned} \quad (2.12)$$

where  $R_{x_1, x_2}(\omega)$  is the cross-spectral density function for the inputs  $x_1(t)$  and  $x_2(t)$ .  $X_1(\omega)$  and  $X_2(\omega)$  are the Fourier transforms of  $x_1(t)$  and  $x_2(t)$ . The expression for the cross-correlation is obtained after computing an inverse Fourier transform as in (2.13) (Lessard, 2006). The delay,  $\hat{\tau}$  is determined by the maximum value in cross-correlation function as shown in Equation (2.14).

$$r_{x_1, x_2}(\tau) = \frac{1}{2\pi} \int_{-\infty}^{\infty} R_{x_1, x_2}(\omega) e^{i\omega\tau} d\omega \quad (2.13)$$

$$\hat{\tau} = \arg \max_{\tau} r_{x_1, x_2}(\tau) \quad (2.14)$$

#### 2.4.4 Generalized Cross-correlation with Phase Transform (GCC-PHAT)

The GCC-PHAT based sound source tracking is the most famous method in the time delay estimation due to a greater advantages of reducing the effects of noise and reverberation (Hosseini *et al.*, 2017; Perez-Lorenzo *et al.*, 2012). The GCC-PHAT method is an extension of normal cross-correlation with added weighting function. The received signals are processed with a hamming window to reduce spectral leakage. In the PHAT, the weighting function of estimating the time delay is expressed as (2.15).

$$\phi(\omega) = \frac{1}{|R_{x_1, x_2}(\omega)|} \quad (2.15)$$

However, the error will be increased if the denominator tends to be zero under the low signal-to-noise ratio (SNR). The time delay estimation based on GCC-PHAT is obtained as shown in Equation (2.16). The block diagram of the TDOA estimation based on GCC-PHAT is shown in Figure 2.4.

$$r_{x_1, x_2}(\tau) = \frac{1}{2\pi} \int_{-\infty}^{\infty} \phi(\omega) R_{x_1, x_2}(\omega) e^{i\omega\tau} d\omega \quad (2.16)$$

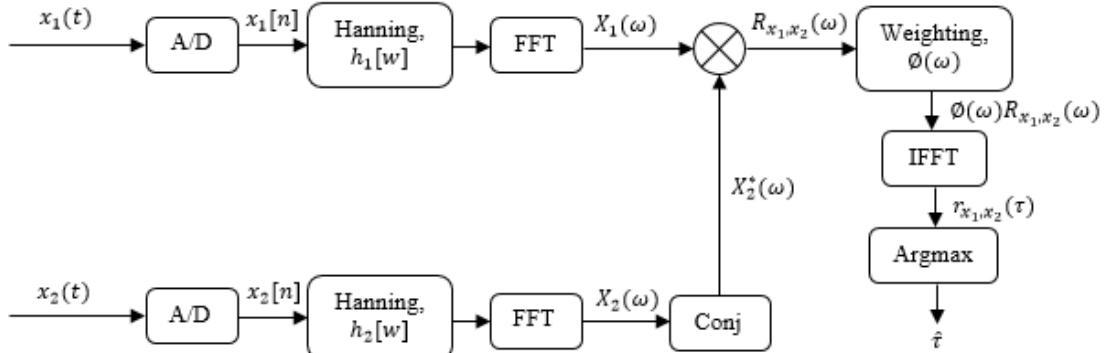


Figure 2.4: Block diagram of the GCC-PHAT function (Hosseini *et al.*, 2017).

## **2.5 Underwater Applications of TDOA**

Several underwater applications such as positioning and localization based on different technologies and methods used are discussed in this section.

### **2.5.1 AUV Underwater Positioning Algorithm Based on Interactive Assistance of Strapdown Inertial Navigation System (SINS) and Long Baseline (LBL)**

A strapdown inertial navigation system (SINS) and a Doppler velocity log (DVL) are the important method to perform the navigation and the tracking of the AUV. It is a device that can provide the vehicle of attitude, velocity and position. The underwater positioning method is based on LBL positioning system. The signal is received from the sound source by an onboard hydrophones. The TDOA estimation based on generalized cross-correlation (GCC) algorithm is implemented to measure time delay of difference. The delay information is obtained after the calculation result of the correlation peak.

The system consist of both navigation and positioning of the AUV as shown in Figure 2.5. It is a combination of an integrated navigation system by using SINS, DVL, magnetic compass pilot (MCP) and LBL in order to solve a multipath effect of the sound signals. The location of hydrophones with velocity, position and heading information of the AUV are considered in calculation to determine the position of vehicle accurately. The result of the TDOA is obtained through the distance between two hydrophones and an equivalent sound velocity of the signals.

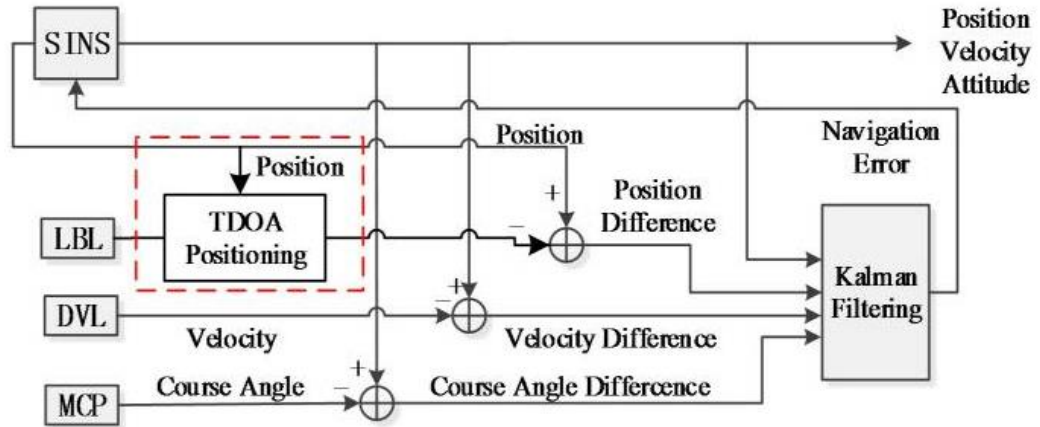


Figure 2.5. Integrated navigation system using SINS, DVL, MCP and LBL (Zhang *et al.*, 2015).

### 2.5.2 Robust Target Tracking with Multi-Static Sensors under insufficient TDOA Information

A multi-static sonar (MSS) system is the target tracking system which involve using the multiple receivers and transmitter. The position of the underwater target is estimated by using the TDOA measurement. A transmitted signal will travel to hit the target and a reflected signal will arrive at the receivers. The time delay measurement is calculated based on Gaussian Mixture Model (GMM) (Song and Mušicki, 2010).

An error of the TDOA measurement is reduced by using a fusion method as shown in Figure 2.6. The intersection lines of an ellipse shape represent the target location. A Gaussian mixture components within an area of intersection are selected in order to compute a fused likelihood. A likelihood value of a selected elements below a threshold value will be terminated. As long as the value of the selected mixture components is greater than the threshold value and the likelihood value is keep at a certain time, it is considered as a true location.

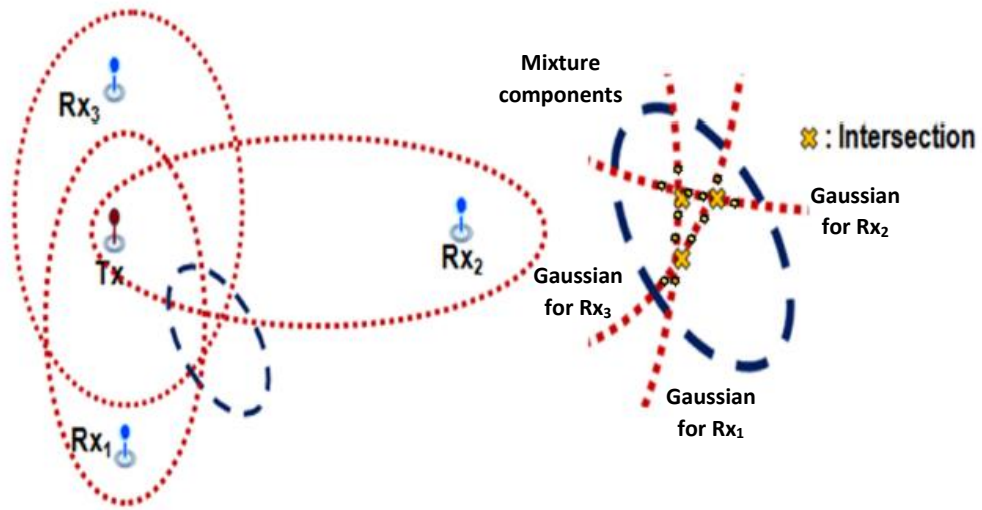


Figure 2.6. Fusion of the TDOA measurement (Shin *et al.*, 2018).

### 2.5.3 A Hybrid Passive Localization Method under Strong Interference with a Preliminary Experimental Demonstration

The target localization is a process of determining the position of the underwater target with a reference to a stationary point. Typically, the position of target that is influenced by a strong interference may lead to an inaccurate TDOA measurement especially when monitoring at ports and harbor areas. This is due to a lot of noise distribution and reflection in these areas. The interference from a container ship is the most significant source in the harbor areas (Jalkanen *et al.*, 2018). The localization system consists of the generalized cross correlation with phase transform (GCC-PHAT) processing and the interference cancellation.

Figure 2.7 demonstrates the difference localization results between two methods, with interference cancellation and without interference cancellation. Obviously, the method with interference cancellation is a correct trajectory of target as compared with another correlation peak is presented in a straight line behavior. Hence, a Radeon transform is a technique used for line detection in order to cancel the



interference. The target source can be localized by the multiple of the TDOA measurement between the hydrophone pairs. However, it may produce an opposite result (target is terminated) if the target signal is weaker than the interference signal.

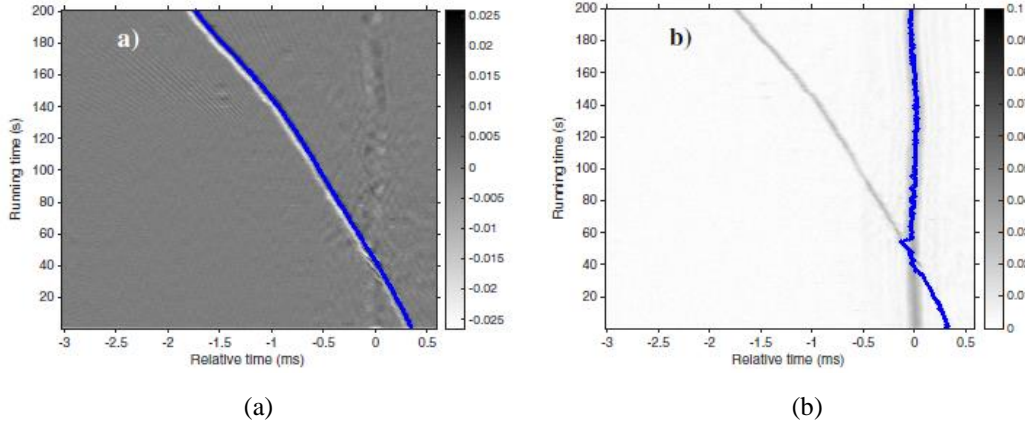


Figure 2.7. Results of localization based on TDOA measurement (a) with interference cancellation, (b) without interference cancellation (Lei *et al.*, 2016).

#### 2.5.4 Time Difference of Arrival Estimation Based on Cross Recurrence Plots, with Application to Underwater Acoustic Signals

Bot *et al.* (2015) proposed a cross-recurrence plots (CRPs) method to perform the TDOA estimation. A recurrence quantification analysis (RQA) is computed on a diagonal parallel to a main diagonal for obtaining a binary matrix from the CRP. A similarity of waveform received by each of hydrophone pairs can be superimposed in order to obtain an alignment of the waveform. When two signals have higher value of the similarity coefficients with given time delay, the TDOA can be estimated based on maximum value of the RQA.

The simulation of the CRP to produce a recurrence plot in a binary image as shown in Figure 2.8. It is a measurement of the similarity between the receiver 1 (reference) and the receiver 2 (translation of signal). 15 black diagonal lines are plotted with a function of an indices. As a result, the TDOA is obtained for lag of 70 samples.

This method is similar with GCC method but it improves the TDOA result in the low signal-to-noise ratio (SNR).

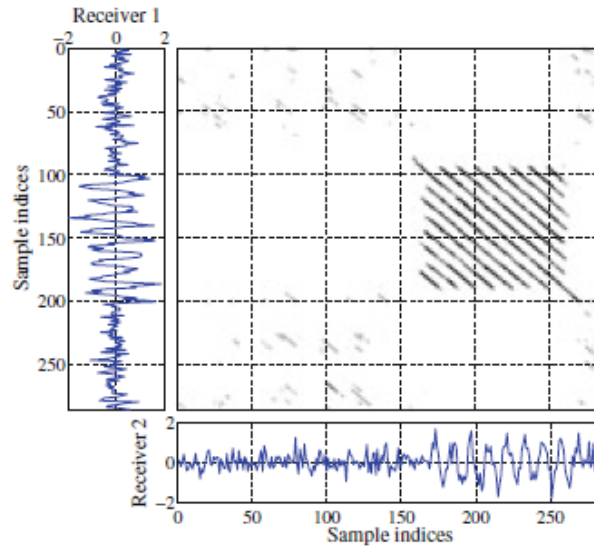


Figure 2.8. TDOA estimation using the CRP matrix (Bot *et al.*, 2016).

### 2.5.5 Performance Improvement of TDOA-based Speaker Localization in Joint Noisy and Reverberant Conditions

In the underwater environment, the noise and reverberation of the acoustic signal leads to the high error of the TDOA measurement. The GCC-PHAT algorithm is modified to improve the accuracy of the TDOA (Abutalebi and Momenzadeh, 2011). The algorithm uses the generalized spectral subtraction method to identify the noise signal. Furthermore, a spherical interpolation or a spherical intersection is a closed form method for TDOA estimation. A primary estimated location of the target source is utilized to figure out the true TDOA.

An outlier of the TDOA leads to an inaccurate position estimation in a 3D. Hence, the outlier removal can be further improved to eliminate a false estimated in the GCC function. A modified algorithm is tested on the real environment with high

noisy input signal. A comparison performance between a maximum likelihood (ML), PHAT and modified PHAT as shown in Figure 2.9. It is obvious that the modified PHAT provides a better performance (robust against noise) than PHAT and ML.

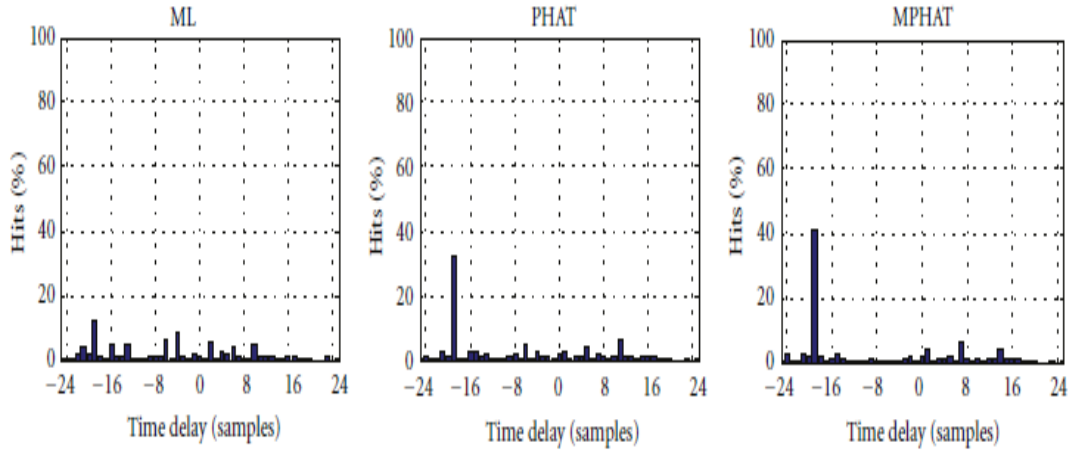


Figure 2.9. Performance of 3D localization in a room (Abutalebi and Momenzadeh, 2011).

### 2.5.6 A TDOA Underwater Localization Approach for Shallow Water Environment

A close loop architecture based on Kalman filter is used to improve the accuracy of positioning (Kouzoundjian *et al.*, 2017). The TDOA is computed by the hydrophone pair that mounted under the boat and a beacon is placed in the low depth. The Doppler frequencies are produced when the boat is moved due to the relative movement between the hydrophones and the beacon. Hence, an amplitude of the correlation will be modulated at code delay and the Doppler frequency function.

The delay Doppler map (DDM) is created and two correlation peaks are detected as shown in Figure 2.10. The information of the DDM is processed by the closed loop tracking system. A prediction of the maximum correlation peak observable by the code delay and the Doppler frequency. Based on Kalman filter, the correlation

is captured by covariance matrix to perform a correction. It helps to reduce the error of peak detection as well as noise reduction.

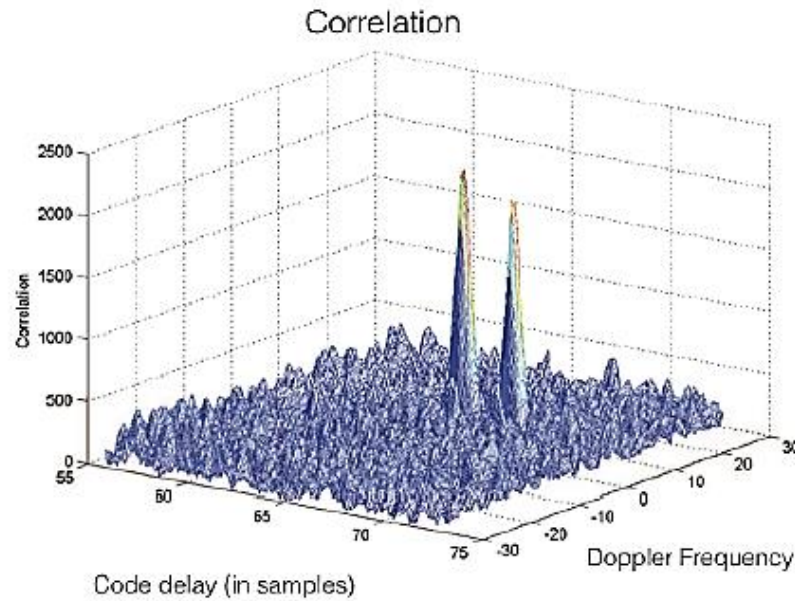


Figure 2.10. Delay Doppler map (3D correlation function) (Kouzoundjian *et al.*, 2017).

### 2.5.7 Moving-Target Position Estimation using GPU-Based Particle Filter for IoT Sensing Applications

In order to achieve the high performance on a large scale computing, a parallel processing is needed to enable fast computations for analyzing data. Hence, the TDOA estimated by using a graphics processing unit (GPU) to accelerate the GCC-PHAT algorithm for processing the multiple of the acoustic signals (Kim *et al.*, 2017). Figure 2.11 shows the parallel fast Fourier transform is computed in the GPU after the signals are received by a sensor array. Then, a particle filter is applied for a non-linear estimation to track a state of the system based on Markov chains.